Journal of Applied Polymer Science

Preparation of heat resisting poly(methyl methacrylate)/graphite composite microspheres used as ultra-lightweight proppants

Tao Chen,[1] Yixia Wang,[1] Chunjie Yan,[1] Hongquan Wang,[1] Yangcheng Xu,[2] Rui Ma[2]

[1]Faculty of Material and Chemistry, China University of Geosciences, Wuhan 430074, China

[2]Engineering Research Center of Nano-Geomaterials of Ministry of Education, China University of Geosciences, Wuhan 430074, China

Correspondence to: C. Yan (E-mail: chjyan2005@126.com) and R. Ma (E-mail: marui.cug@gmail.com)

ABSTRACT: Ultra-lightweight heat resisting poly(methyl methacrylate) (PMMA)/graphite microspheres were successfully prepared via *in situ* suspension polymerization. The Fourier transform infrared and X-ray powder diffraction results confirmed the successful preparation of the composite microspheres. Field emission scanning electron microscope analysis illustrated that the graphite particles were dispersed in microspheres and the PMMA/graphite composite microspheres had good sphericity and roundness. Furthermore, density analysis indicated that the apparent density of composites microspheres was about 1.055–1.135g/cm^3 which was suitable for the transmission with water carrying. The results from thermodynamic test revealed that the thermal stability of the composite was significantly improved with increasing graphite content, which could be used as ultra-lightweight proppant in deep underground. In addition, the crushing rate decreased to 0.5% with graphite ratio of 3.0% at the pressure of 69 MPa. Therefore, PMMA/Graphite composite microspheres exhibit a promising application in petroleum or gas exploitation as water carrying fracturing proppants. © 2015 Wiley Periodicals, Inc. J. Appl. Polym. Sci. **2015**, *132*, 41924.

KEYWORDS: composites; functionalization of polymers; gas; oil

Received 30 September 2014; accepted 29 December 2014

DOI: 10.1002/app.41924

INTRODUCTION

Hydraulic fracturing is an effective and commonly used way to enhance petroleum or gas operation in oilfields.[1,2] Proppants, required in hydraulic fracturing operations, is used for supporting the hydraulic fractures and keeping them open against the application of closure stresses to ensure conduction of oil and gas to the borehole.[3] The ideal properties of the proppant must have high strength as diamond, light as water, and cheap as earth. What's more, properties of high sphericity, acid resistance, and low turbidity are also important for proppants. But, it is difficult to get one product with all these ideal properties.[4] Proppants used in oil industry include sand, glass beads, walnut hulls, and metal shot as well as resin-coated sands, intermediate strength ceramics, and sintered bauxite, which has the ability to effectively withstand the respective reservoir closure stress environment.[5] The relative strength of these various materials increases with their corresponding apparent specific gravity (ASG), typically ranging from 2.65 g/cm^3 for sands to 3.4 g/cm^3 for sintered bauxite.[6] Difficult proppants transport and reducing fracture conductivity might be caused with increasing ASG.[7,8] More recently, ultra-lightweight (ULW) materials have been used as proppants since they reduced the required fluid velocity for proppant transport within the fracture,[9–11] which provided a greater number of fracture area to increase the fracture conductivity. Representative of such proppants are significantly lighter deformable particles.

Poly(methyl methacrylate) (PMMA) microsphere is a kind of functional material which has high sphericity, high compressive strength, and ULW (close to 1 g/cm^3).[12] However, PMMA shows a poor thermal stability and high cost, which limits its wide applications. On the contrary, graphite exhibits excellent thermal stability, it can efficiently improve the mechanical properties and thermal stability of polymer matrix.[13–15] Hence, the introduction of graphite into PMMA matrix is an efficient approach to possess the merits of both organic and inorganic phases. In the early studies, PMMA/graphite composite particles and their performances have been reported in several literatures.[16,17] However, to our knowledge, there are still no reports about the application of PMMA microspheres in ULW proppant.

In the present work, ULW PMMA/graphite composite microspheres with high sphericity, high compressive strength, acid resistance, thermal stability, and low turbidity were prepared via

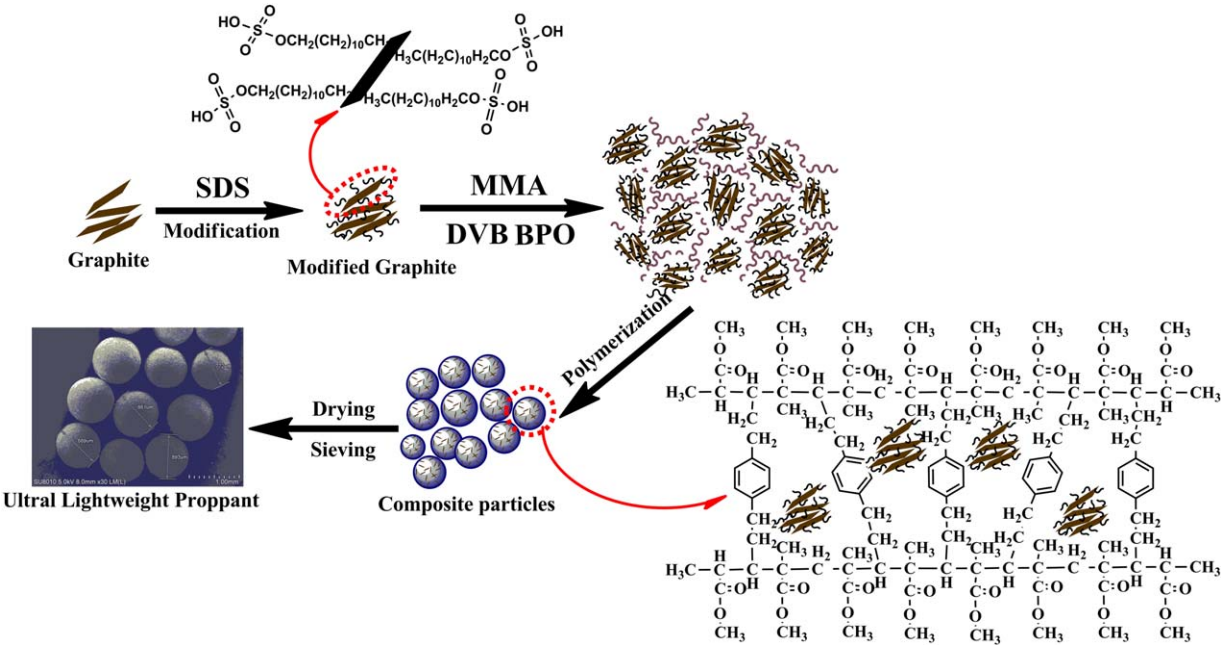

Figure 1. Schematic illustration of the synthesis process of ultra lightweight proppant. [Color figure can be viewed in the online issue, which is available at wileyonlinelibrary.com.]

in-situ suspension polymerization, which would exhibit a promising application to petroleum or gas exploitation as water carrying fracturing proppants.

EXPERIMENTAL

Materials

Graphite powder was purchased from Sinopharm Chemical Reagent Co., Ltd, China; Methyl methacrylate (MMA, 99 wt %, Sinopharm Chemical Reagent Co., Ltd, China) was treated with 5% sodium hydroxide solution to remove the inhibitor and then distilled under a reduced pressure; Divinylbenzene (DVB, $[m_{DVB}]/[p_{DVB}] = 92/8$; Tianjin Fuchen Chemical Regents Factory, China) and benzoyl peroxide (BPO, Tianjin Damao Chemical Regents Factory, China) were used as cross-linking agent and initiating agent, respectively. Magnesium chloride ($MgCl_2$), sodium hydroxide (NaOH), and methanol were purchased from Sinopharm Chemical Reagent Co., Ltd (China). Sodium dodecyl sulfates (SDS) was purchased from Tianjin Fuchen Chemical Regents Factory (China) and methanol was purchased from Sinopharm Chemical Reagent Co., Ltd (China). Quartz sand (20–40 mesh) and ceramic (20–40 mesh) were got from Shanghai Jin Yuan quartz sand Ltd. (China) and Yixing Orient Petroleum Proppant Co., Ltd., respectively.

Preparation of Modified Graphite

To prepare the modified graphite, 2 g SDS and 200 mL deionized (DI) water were poured into a four-necked round-bottomed flask equipped with a thermometer, a funnel, a reflux condenser, and a mechanical stirrer in an oil bath at 85°C. After the SDS solution dissolved, 20 g graphite was added into the solution, and then the graphite mixture was stirred for another 4 h with a mechanical stirrer. Then the resultant graphite was centrifuged and dried at 70°C for 12 h to obtain the modified graphite.

Preparation of PMMA/Graphite Composite Microspheres via *In Situ* Suspension Polymerization

PMMA/graphite composite microspheres were synthesized through *in situ* suspension polymerization. A typical preparation procedure was described as follows. Firstly, 1.6 g NaOH and 4.0 g $MgCl_2 \cdot 6H_2O$ were replaced into 120 mL DI water at 60°C with a vigorous stirring. After that, 0.3 g BPO and 3.0 g DVB were dissolved in 20.0 g MMA, then a stipulated amount of graphite was added. Finally, the mixture was heated to 80°C and kept for 1 h, then at 80°C for 2 h, followed by boiling at 90°C for 2 h. After that the aqueous phase was removed; black microspheres were obtained and then washed with water and methanol, orderly. For comparison, microspheres without graphite were fabricated under the same condition. The obtained microspheres were divided into different mesh specifications, which were 10–20 mesh, 20–40 mesh, 40–60 mesh, and 60–80 mesh, respectively. The microspheres of 20–40 mesh (the most common size of proppants) were used as research object here.

Characterizations

The Fourier transform infrared (FTIR) spectra of particles were obtained by means of a Nicolet Avatar 360 FTIR spectrometer in the range 400–4000 cm^{-1} using the KBr pellet technique. Dispersion stability of graphite was reflected through transmittance test by Visible Spectrophotometer (722N, Shanghai Precision & Scientific Instrument Co., Ltd.) at 540 cm^{-1}. The surface morphology and microstructure of these samples were performed with field emission scanning electron microscope (FE-SEM, Hitachi SU8010). X-ray powder diffraction (XRD) was recorded on a Rigaku Multiflex powder diffract meter with Cu radiation between 5° and 70° with a scan rate of 0.5°/min and incident wavelength of 0.154056 nm (Cu $K\alpha$). The density was calculated by the ratio of mass to volume. Thermal behavior of composite particles was

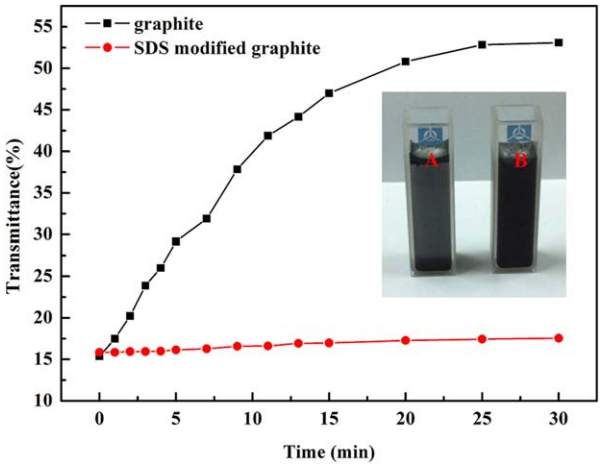

Figure 2. Transmittance of original graphite (A) and SDS modified graphite (B) disperse in water. [Color figure can be viewed in the online issue, which is available at wileyonlinelibrary.com.]

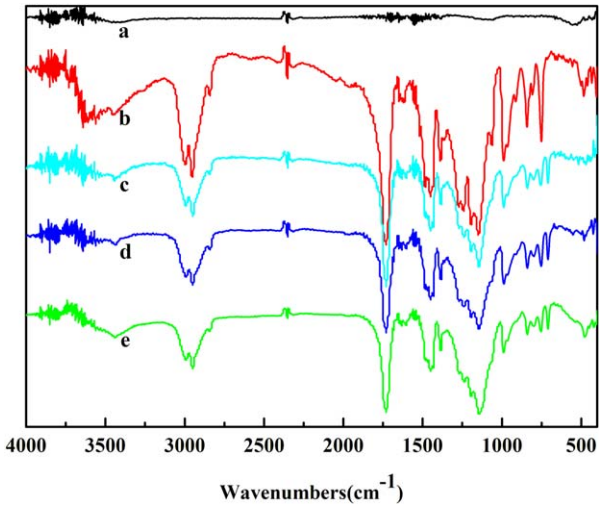

Figure 3. FTIR spectra of (a) raw graphite, (b) pure PMMA, (c) PMMA/graphite (1.0 wt %), (d) PMMA/graphite (3.0 wt %), (e) PMMA/graphite (5.0 wt %). [Color figure can be viewed in the online issue, which is available at wileyonlinelibrary.com.]

studied with thermogravimetric analysis (TGA, STA409PC, Netzsch, Germany) by a Diamond calorific analyzer of Perkin Elmer. The compressive strength was performed on WAW100D microcomputer-controlled electro-hydraulic servo universal testing machine (Jinan Hengsi Instruments Co., Ltd). The tests of acid solubility and turbidity were determined by the Chinese Petroleum and Gas Industrial Standard (SY/T 5108-2006).

RESULTS AND DISCUSSION

Proposed Mechanism for the Preparation of ULW Proppants

According to the experimental procedure, a possible mechanism for the preparation of ULW proppants was illustrated in Figure 1. Here, the main challenge was to introduce the graphite with poor chemical activity into PMMA. Firstly, graphite was modified by the anionic surfactant (SDS) to keep the hydrophobic end toward the surface of the graphite. The SDS molecule has a tail of 12 carbon atoms attached to a sulfate group, giving the molecule amphiphilic properties: the hydrophobic group, $-CH_3$, of the SDS molecule, adsorbs on the surface of graphite, while the hydrophilic head, $-SO_4$, associates with water for dissolution.[18] This enhanced the compatibility between the graphite and MMA. During polymerization, anchoring sites on the graphite for MMA was provided due to Brownian motion. It is possible that the anchor of the PMMA particles is owing to the weak Van der Waals force originating from the random contact of carbon atoms and PMMA chain. The attachment of PMMA composite microspheres to the graphite becomes possible and does not cause the selective anchoring of all PMMA composite microspheres.[19,20] The unanchored PMMA latex was removed by successive washing in methanol to get the PMMA/graphite composite microspheres. Finally, ULW proppants were obtained after being dried and sieved.

Dispersion Stability of Graphite Before and After Modified

Dispersion stability of graphite in water has been systematically studied by Vis spectrophotometer. The transmittance changes over time to reflect the stability of the graphite dispersed in water. The better the graphite disperse in water the smaller transmittance it shows.[21] Figure 2 showed the dispersion stability of original graphite before and after modified in aqueous solution. As shown in Figure 2, the transmittance of original graphite dispersed in water significantly increased with the standing time, due to the settlement of graphite. After modified by SDS, the transmittances of modified graphite dispersed in water slightly increased with the standing time. It could be explained that the more SDS attached on the surface of graphite, the more stable graphite dispersed in water, and the lower transmittance. Digital picture of the original graphite dispersion diluted by a factor of about 0.1 mg mL^{-1} (vial A) and the same dispersion after modified by SDS by the same factor (vial B) showed the original graphite dispersion diluted stratified: Part of the graphite particles floated up and part of the graphite

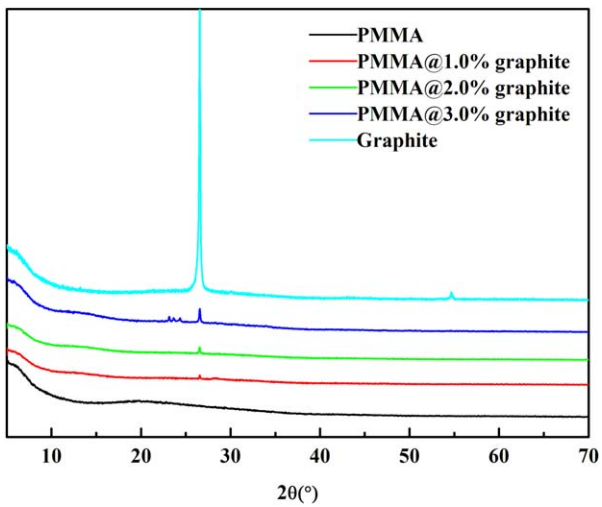

Figure 4. XRD patterns of raw graphite, pure PMMA, PMMA/1.0 wt % graphite, PMMA/3.0 wt % graphite and PMMA/5.0 wt % graphite. [Color figure can be viewed in the online issue, which is available at wileyonlinelibrary.com.]

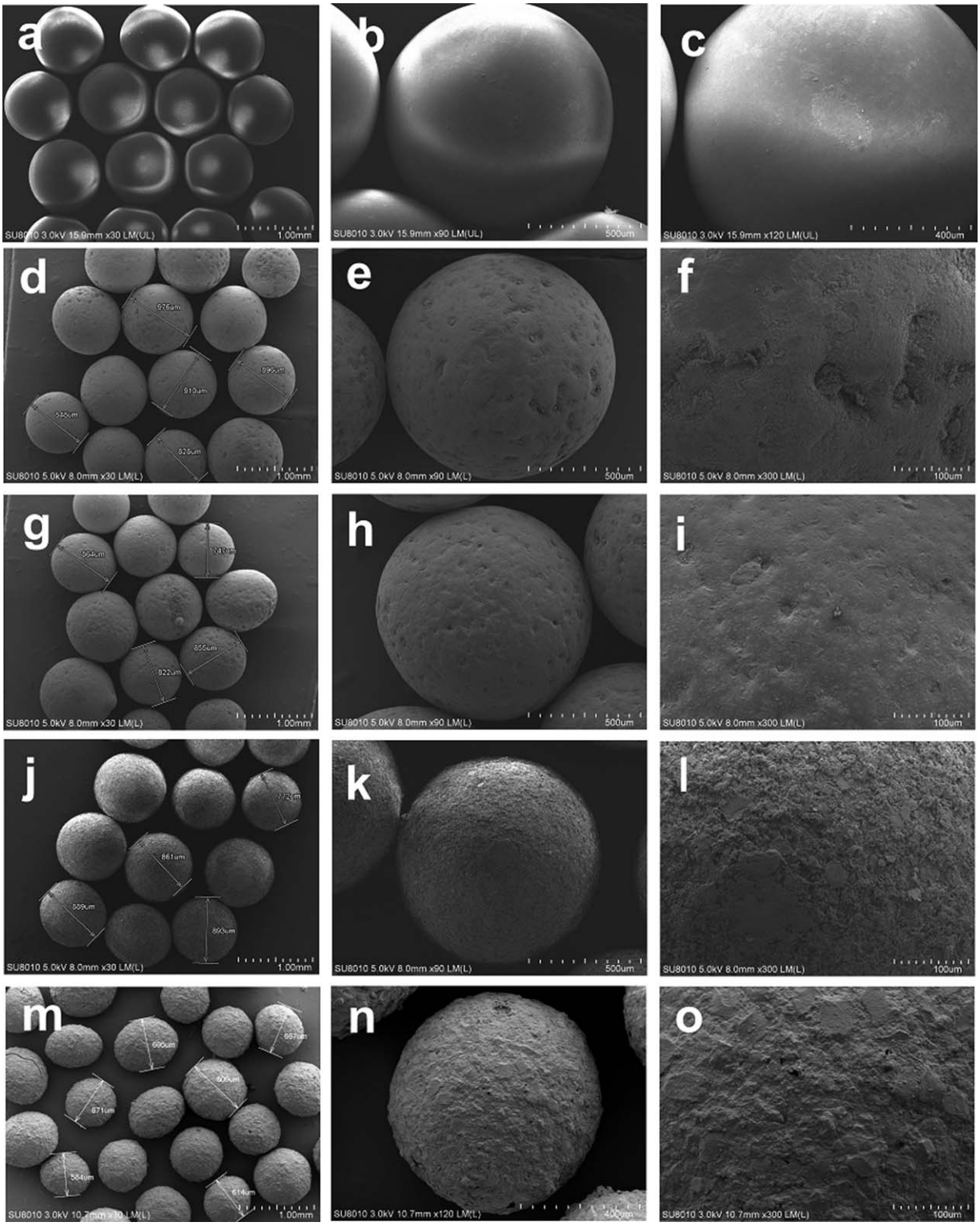

Figure 5. SEM images of pure PMMA microspheres (a–c) and composite microspheres: (d–f) PMMA/graphite composite microspheres (1.0 wt %); (g–i) PMMA/graphite composite microspheres (3.0 wt %); (j–l) PMMA/graphite composite microspheres (5.0 wt %); ceramic (m–o).

particles settlement to the bottom. But the graphite evenly dispersed in the water after modified by SDS. The transmittance results further demonstrates that experimental condition was better for preparing PMMA/graphite microspheres.

FTIR Spectra Analysis

To verify whether the graphite had been doped into PMMA or not, the FTIR spectra of raw graphite, pure PMMA and PMMA/graphite (1.0 wt %; 3.0 wt %; 5.0 wt %) composite

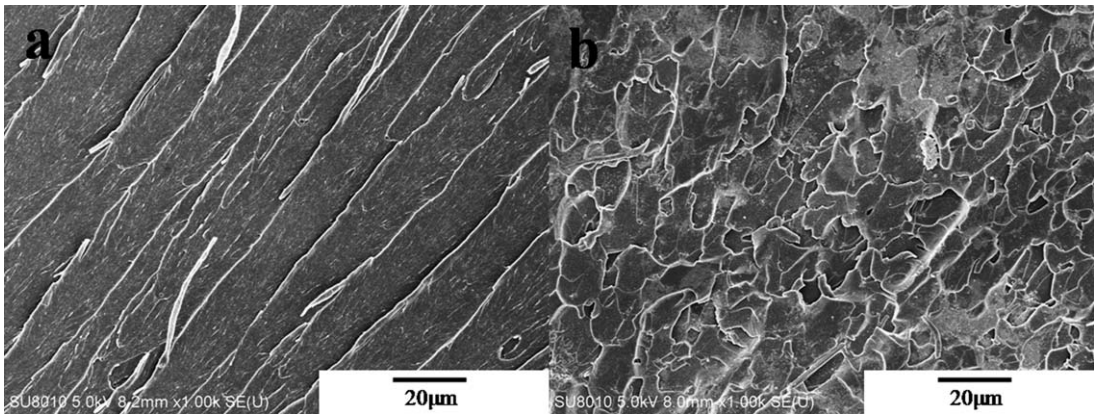

Figure 6. SEM images of section for pure PMMA (a) and PMMA/graphite (3 wt %) composite particles (b).

microspheres were shown in Figure 3. From the spectra of pure PMMA [Figure 3(b)] and PMMA/graphite [Figure 3(c–e)], the characteristic peak of —C═O in carbonyl groups of PMMA at 1731 cm^{-1} was clear in PMMA/graphite composites. The two C—H stretching peaks at 2952 cm^{-1} and 2995 cm^{-1} appear both in the spectra of Figure 3(b) and Figure 3(c–e). The peaks at 1454 cm^{-1} and 1390 cm^{-1} in Figure 3(b) and Figure 3(c–e) are attributed to the vibration mode of —CH_2 or —CH_3 group in PMMA.[22] The peaks at 1000–1200 cm^{-1} are attributed to the stretching vibration of the C—O group of PMMA. In addition, in the range of 2600–3300 cm^{-1}, a broad and strong —OH absorption band appears, at the same time, the peaks at 1706–1720 and 1210–1320 cm^{-1} are attributed to the stretching vibration of C═O and C—O, respectively. All these characteristics indicate the presence of the —COOH group. Compared with the spectrum of pure PMMA, the spectrum of PMMA/graphite composite microsphere [Figure 3(c)] at 1450–1650 cm^{-1} arose sight offsets and the intensity of the peak at 698 cm^{-1} was obviously weakened, which was contributed to the interaction between PMMA and graphite.[23] Furthermore, compared with the raw graphite [Figure 3(a)], the characteristic peaks in the spectra of pure PMMA and PMMA/graphite do not appear in the curve of raw graphite, implying the successful preparation of PMMA/graphite composite particles.

XRD Results

Figure 4 illustrated the XRD patterns of pure PMMA, graphite and PMMA/graphite composite in the 2θ range between 5° and 70°. In the diffract gram of pure PMMA, there is no sharp diffraction peaks, confirming the non-crystalline nature. PMMA is known to be an amorphous polymer.[24,25] The graphite pattern reveals an intense and sharp peak located at $2\theta = 26.38°$, corresponding to the characteristic diffraction peak of graphite powder.[25] After the introduction of graphite into PMMA matrix, the peak at $2\theta = 26.38°$ appears, and it becomes intense and sharp with the increase of graphite added amount. Due to the interaction between PMMA and graphite, the intensity changes in the composite particle and some small peaks are situated in the diffract gram. The higher intensity for higher graphite content can be attributed to the higher number of graphite layers.[26] Therefore, it is demonstrated that the graphite are fully exfoliated and randomly dispersed in the polymer matrix. As a result, the crystallinity of the PMMA is largely influenced by graphite–PMMA–graphite particle. This further indicates that the structures of the graphite have not changed in the composite.

Morphology and Properties of PMMA/Graphite Composite Microspheres

The morphology of the pure PMMA microspheres, ceramic, and PMMA/graphite (1.0 wt %; 3.0 wt %; 5.0 wt %) composite microspheres were shown in SEM images (Figure 5). The surface of pure PMMA microspheres [Figure 5(a–c)] was very smooth and it was turned rougher with increasing the amount of graphite. Especially, for the higher magnification [Figure 5(f,i,l)]. Obvious difference was found due to slight crease of flexible and ultrathin graphite, looking like creased scales. This provided direct visual evidence that the graphite was successfully doped into the PMMA microsphere during polymerization.[27,28] For comparison, the SEM images of ceramics under different magnification were presented in Figure 5(m,n,o), which showed a rough surface and a bad sphericity to the composite microspheres.

It could be seen from the sections of pure PMMA [Figure 6(a)] and PMMA/graphite (3.0 wt %) composite particles [Figure

Table I. The Basic Performance of ULW Proppant and Conventional Proppant

	ULW proppant							
The amount of graphite (%)	0.0	1.0	2.0	3.0	4.0	5.0	Quartz sand	Ceramic
Sphericity	>0.9	>0.9	>0.9	>0.9	≥0.9	≥0.9	0.65	0.85
Roundness	>0.9	>0.9	>0.9	>0.9	≥0.9	≥0.9	0.65	0.85
Acid solubility (%)	0.08	0.09	0.08	0.09	0.06	0.05	4.59	5.89
Turbidity (FTU)	15	35	50	58	64	75	100	80

6(b)] that the internal structure of pure PMMA was compact, while abundant homogeneously scales were observed inside the composite particles. This illustrated that the graphite particles were dispersed in the microspheres evenly, which made a great contribution to the heat resisting and thermal stability characteristic of composite particles.[29]

The measurement of sphericity, roundness, acid solubility, and turbidity were qualitatively measured according to the standards of ISO 13503-2. The results of the sphericity, roundness, acid solubility, and turbidity of PMMA/graphite composite microspheres with different content of graphite were shown in Table I. From the table, the sphericity and roundness of PMMA/graphite composite microspheres were above 0.9, which were obviously better than quartz sand (0.65) and ceramic (0.85). Good sphericity and roundness provide the high proppant-pack porosity, leading to the increase of permeability at higher stresses with little effect from temperature. Meanwhile the perfect sphericity can improve the flow conductivity of proppant.[6,30] The acid solubility of PMMA/graphite composite microspheres was close to zero which was obviously better than quartz sand (4.59%) and ceramic (5.89%). The lower acid solubility illustrated the better stability of the proppant in an acidic environment, which means that the proppants could provide long-term conductivity.[31] The turbidity of PMMA/graphite composite microspheres was much lower than quartz sand (100 FTU) and ceramic 80 FTU). Turbidity was caused by tiny crisp crumbs, which would fill the gap between the proppants and decrease the conductivity.[32] So the high sphericity and roundness, low acid solubility and turbidity of PMMA/graphite composite microspheres exhibited a promising application as ULW proppant.

The Densities of PMMA/Graphite Composite Microspheres

In order to adapt to the working environment of oil field as water carrying fracturing proppants, composite particles needed to be ULW. From the test, the measurements of apparent density (ρ_A) included the internal porosity of particles as part of the particle volume. They were measured in water and determined in accordance with the Petroleum and Gas Industrial Industry Standard (SY/T 5108-2006) of China and calculated based on this formula:

$$\rho A = \frac{M_s}{V_s} \times 100\% \quad (1)$$

where M_s and V_s are the weight and the volume of the PMMA/graphite composite particles, respectively.

Figure 7 represented the density of pure PMMA microspheres and PMMA/graphite composite microspheres. It could be seen that the densities of composite microspheres increased from 1.055 to 1.135 g/cm^3 when the graphite content was raised to 5%. According to the reports in the literature,[30,31] the densities of conventional proppants-quartz sand and ceramic were 2.65 and 3.25 g/cm^3, respectively. It could be explained that since the density of graphite powder is higher than that of pure PMMA, when they were blended the density of composite particles is between both components, and increased with increasing graphite content.[28] What's more, the density of traditional ULW proppant, such as resin coated and impregnated ground walnut hull and porous ceramic particle coated (not impregnated) by

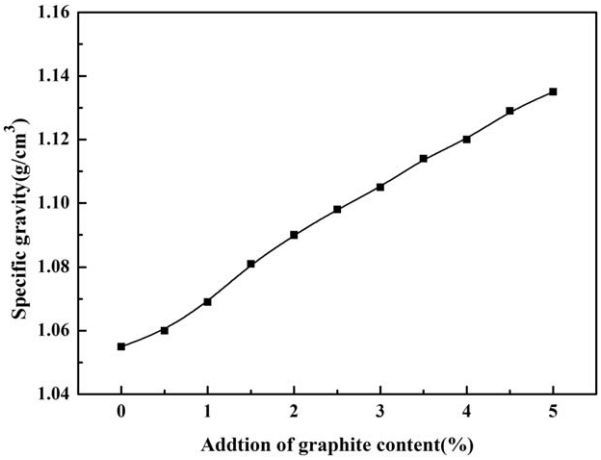

Figure 7. Densities of PMMA/graphite composite microspheres.

resins,[32,33] were 1.25 and 1.75 g/cm^3, respectively. Thickening agents, such as guar gum were needed in the fracturing fluid by using conventional high-density hydraulic fracturing proppants,[34] which are contaminative and hard to be degraded. Compared with conventional high-density proppants, if the above composite microspheres could be used as ULW proppant in water fracturing, the damage caused by traditional hydraulic fracturing can be avoided and the fracturing cost will be reduced.

Thermal Behaviors of PMMA/Graphite Composite Microspheres

The thermal properties of these composite microspheres were evaluated by TGA. Figure 8 showed the TGA curves of PMMA, PMMA/1.0 wt % graphite, PMMA/3.0 wt % graphite, PMMA/5.0 wt % graphite at a heating rate of 10°C/min under nitrogen flow. From the TGA curve, the thermal stabilities of the PMMA/graphite composite particles were initially better than that of pure PMMA. For pure PMMA, the onset temperature is 268°C, while for the composites it increases to 285°C for PMMA/1.0 wt % graphite, 327°C for the PMMA/3.0 wt %

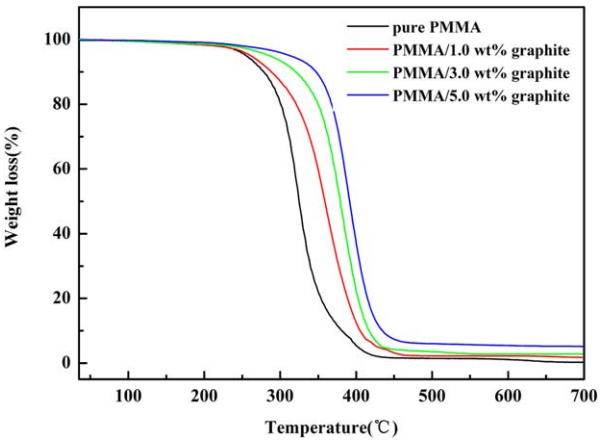

Figure 8. TGA curves of PMMA, PMMA/1.0 wt % graphite, PMMA/3.0 wt % graphite, PMMA/5.0 wt % graphite at a heating rate of 10°C/min under nitrogen flow. [Color figure can be viewed in the online issue, which is available at wileyonlinelibrary.com.]

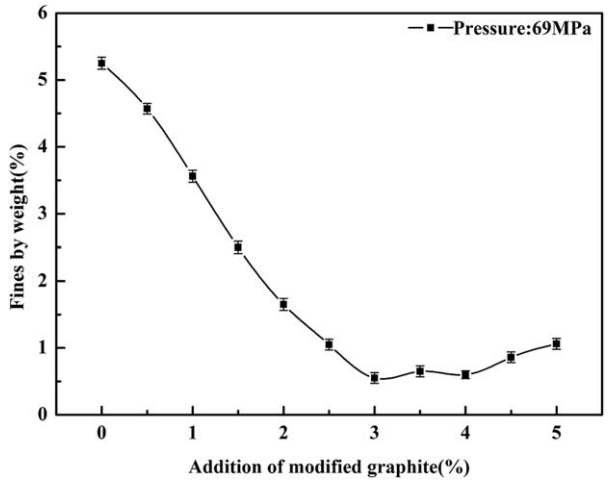

Figure 9. Percentage of damage of PMMA/graphite composite microspheres under the pressure of 69 MPa.

graphite, and 345°C for the PMMA/5.0 wt % graphite. As the graphite content of the hybrid increased, the temperature at which the weight drastically decreased and the plateau region appeared was increased. Moreover, around 400°C, at which temperature residual PMMA was completely degraded, the copolymers showed higher residual weights than their graphite contents. This phenomenon might be attributed to the interpenetration of polymer chains with an inorganic scaffold of graphite which could restrain the mobility of the polymer chains.[35] In view of these results, the high graphite content of the composite particles could enhance the thermal stability of composite particles dramatically. Therefore, the incorporation of the graphite platelet resulted in pronounced improvement in thermal stability.

Compression Tests

Taking into account of the working environment of fracturing proppant, the most important properties of proppants are excellent compressive strength. Confined compression tests were carried out following the American Petroleum Institute (APIRP 60) standard on proppant.[36] According to the reference standard, the fines of weight of composite particles under the pressure of 69 MPa were chosen, and the detailed results were depicted in Figure 9. The crushing rate increased firstly and then decreased with increasing graphite content. And the percentage of damage decreased to 0.5% with the addition of 3.0% graphite, while the graphite content raised to 5%, the percentage of damage increased to about 1.1%. The observed compressive behavior could be explained by the plasticizing action of small molecules on the polymer. Graphite behaved as the flexibilizer, then leaded to the good mechanical properties if they were presented in small amounts and distributed homogeneously in the PMMA microspheres.[37] However, because of the poor compatibility of graphite, this could lead to inhomogeneous distribution, poor adhesion, increasing brittleness of composites and the decreasing compressive strength as the proportion of graphite increased.[6,38] According to the literature, under the same condition, the fragmentation rate of quartz sand was 36% and ceramic was 10.2%.[39] Therefore, the traditional proppants may be replaced by composite microspheres which were more suitable as water carrying fracturing proppant.

CONCLUSION

In this study, PMMA/graphite composite microspheres which were aimed to be used as ULW proppants were successfully prepared via *in-situ* suspension polymerization technique. The optimum conditions for the synthesis of PMMA/graphite composite microspheres and the effect of graphite content on the compressive strength, density, thermal stability of PMMA/graphite microspheres were investigated. The results revealed that the technique of *in-situ* suspension polymerization was feasible for the preparation of the PMMA/graphite composite microspheres. The optimal dosage of graphite was 3.0 wt %. Under this condition, composite microspheres has a good sphericity (0.9), low-density (1.099 g/cm^3), high thermal stability, low acid solubility close to zero, low turbidity (<80). Therefore, PMMA/graphite composite microspheres exhibited a promising application as water carrying fracturing proppant.

ACKNOWLEDGMENTS

This work was supported by Public Service Project of the Chinese Ministry of Land and Resources (201311024) and the National Natural Science Foundation of China (41372367).

REFERENCES

1. Barati, R.; Liang, J. *J. Appl. Polym. Sci.* **2014**, *131*, 16.
2. Marongiu-Porcu, M.; Economides, M. J.; Holditch, S. A. *J. Nat. Gas. Sci. Eng.* **2013**, *14*, 91.
3. Wu, T.; Wu, B.; Zhao, S. *Mater. Lett.* **2013**, *92*, 210.
4. Bortolan, N. L.; Andrei, K. *Int. J. Rock. Mech. Min.* **2013**, *61*, 223.
5. Duenckel, R.; Conway, M. W.; Eldred, B.; Vincent, M. C. *Spe. Prod. Oper.* **2012**, *27*(02), 131.
6. Han, X.; Cheng, Q.; Bao, F.; Gao, J.; Yang, Y.; Chen, T.; Ma, R. *Polym.-Plast. Technol.* **2014**, *53*, 1647.
7. Kulkarni, M. C.; Ochoa, O. O. *Compos. Sci. Technol.* **2012**, *72*, 879.
8. Gaurav, A.; Dao, E. K.; Mohanty, K. K. *J. Petrol. Sci. Eng.* **2012**, *92*, 82.
9. Deng, S.; Li, H.; Ma, G.; Huang, H.; Li, X. *Int. J. Rock. Mech. Min.* **2014**, *70*, 219.
10. Khanna, A.; Kotousov, A.; Sobey, J.; Weller, P. J. *Petrol. Sci. Eng.* **2013**, *100*, 9.
11. Alan, R. R.; Harold, D. B.; William, D. W.; Christopher, J. S. *Spe. Prod. Oper.* **2006**, *21*(2), 212.
12. Nishiura, T.; Abe, Y.; Kitayama, T. *Polym. J.* **2010**, *42*(11), 868.
13. Yu, L.; Yao, L.; You, J.; Guo, Y.; Yang, L. J. *Appl. Polym. Sci.* **2014**, *131*, 1.
14. Sengupta, R.; Bhattacharya, M.; Bandyopadhyay, S.; Bhowmick, A. K. *Prog. Polym. Sci.* **2011**, *36*(5), 638.
15. Shalwan, A.; Yousif, B. F. *Mater. Design.* **2014**, *59*, 264.

16. Xu, K.; Erricolo, D.; Dutta, M.; Stroscio, M. A. *Superlattice. Microst.* **2012**, *51*(5), 606.
17. Swain, S. K.; Prusty, G.; Ray, A. S.; Behera, L. *J. Exp. Nanosci.* **2014**, *9*(3), 240.
18. Duan, W. H.; Wang, Q.; Collins, F. *Chem. Sci.* **2011**, *2*, 1407.
19. Zheng, Z.; Li, W.; Sun, H. *Polym. Compos.* **2013**, *34*, 1110.
20. Patole, A. S.; Patole, S. P.; Kang, H. *J. Colloid Interface Sci.* **2010**, *350*, 530.
21. Yan, J. T.; Miao, X. J.; Zhang, Q. Y.; Cui, X. J.; Li, J. F.; Wang, H. Y. *Polym. Eng. Sci.* **2011**, *51*, 294.
22. Hashizume, M.; Nagasawa, Y.; Suzuki, T.; Kawashima, S.; Kamitakahara, M. *Colloids Surf. B: Biointerfaces* **2011**, *84*, 545.
23. Ye, L.; Meng, X. Y.; Ji, X.; Li, Z. M.; Tang, J. H. *Polym. Degrad. Stabil.* **2009**, *94*(6), 971.
24. Wang, W.; Liu, Y.; Li, X.; You, Y. *J. Appl. Polym. Sci.* **2006**, *100*(2), 1427.
25. Meneghetti, P.; Qutubuddin, S.; Webber, A. *Electrochim. Acta* **2004**, *49*, 4923.
26. Yasmin, A.; Luo, J. J.; Daniel, I. M. *Compos. Sci. Technol.* **2006**, *66*(9), 1182.
27. Li, Y.; Wang, Z.; Yang, L. *Chem. Commun.* **2011**, *47*, 10722.
28. Qin, Q.; Zhong, Y.; Cheng, J. *J. Appl. Polym. Sci.* **2013**, *129*, 3482.
29. Yang, Y.; Diao, M.; Gao, M.; Sun, X.; Wang, S. *Electrochim. Acta* **2014**, *132*, 496.
30. Neto, J.; Abrahao, T.; Prata, F. G. M.; Gomez, J.; Pedroso, C. A.; Martins, M.; Silva, D. N. *Spe. Drill. Completion* **2012**, *27*(04), 613.
31. Wu, T.; Wu, B.; Zhao, S. *Mater. Lett.* **2013**, *92*, 210.
32. Kulkarni, M. C.; Ochoa, O. O. *Mech. Adv. Mater. Struct.* **2012**, *19*(1-3), 109.
33. Rightmire, C. M.; Leshchyshyn, T. T.; Vincent, M. C. In SPE Annual Technical Conference and Exhibition. Society of Petroleum Engineers, 2005, January.
34. Brannon, H. D.; Malone, M. R.; Rickards, A. R.; Wood, W. D.; Edgeman, J. R.; Bryant, J. L. In SPE Annual Technical Conference and Exhibition. Society of Petroleum Engineers, 2004, January.
35. Inuwa, M. I.; Hassan, A.; Samsudin, A. S.; Mohamad Haafiz, M. K.; Jawaid, M.; Majeed, K. *J. Appl. Polym. Sci.* **2014**, *131*, 15.
36. Kulkarni, M. C.; Ochoa, O. O. *Compos. Sci. Technol.* **2012**, *72*(8), 879.
37. Sengupta, R.; Bhattacharya, M.; Bandyopadhyay, S.; Bhowmick, A. K. *Prog. Polym. Sci.* **2011**, *36*(5), 638.
38. Yasmin, A.; Luo, J. J.; Daniel, I. M. *Compos. Sci. Technol.* **2006**, *66*(9), 1182.
39. Zhang, W. M.; Li, Z. T. *Oilfield Chem.* **2013**, *30*, 189.